

In-Situ Measurements of Cirrus Clouds on a Global Scale

G. Lloyd^{1,2}, M. Gallagher¹, T. Choularton¹, M. Krämer³, P. Andreas⁴, D. Baumgardner⁵

¹Centre for Atmospheric Science, University of Manchester, Manchester, M13 9PL, UK.

²National Centre for Atmospheric Science, Manchester, M13 9PL, UK.

³Forschungszentrum Jülich, IEK-7 Stratosphere, Jülich, Germany.

⁴Forschungszentrum Jülich, IEK-8 Troposphere, Jülich, Germany

⁵Droplet Measurement Technologies, Boulder, CO, USA.

Corresponding author: Gary Lloyd (gary.lloyd@manchester.ac.uk)

Key Points:

- Global in-situ measurements of high altitude cirrus clouds are presented with a focus on 6 regions to identify seasonal trends in cloud fractions.

Abstract

Observations of high-altitude cirrus clouds are reported from measurements made during routine monitoring of cloud properties on commercial aircraft as part of In-Service Aircraft for a Global Observing System. The global scale of the measurements is revealed, with 7 years of in-situ data producing a unique and rapidly growing dataset. We find cloud fractions measured ≥ 10 km at aircraft cruise altitude are representative of seasonal trends associated with the mid latitude jet stream in the northern hemisphere, and the relatively higher cloud fractions found in tropical regions such as the Inter-Tropical Convergence Zone and South East Asia. The characteristics of these clouds are discussed and the potential different formation mechanisms in different regions assessed.

1 Introduction

In-Service Aircraft for a Global Observing System (IAGOS) is a European Research Infrastructure that combines the scientific expertise of its member institutions with the infrastructure of civil aviation to make near continuous measurements of the atmosphere on a global scale. The history of measurements on commercial aircraft dates back to 1994 through the Measurement of Ozone and Water Vapour on Airbus Aircraft (MOZAIC) and from the 2008 Civil Aircraft for the Regular Investigation of the Atmosphere Based on an Instrument Container (CARIBIC). From this, IAGOS-CARIBIC and IAGOS-CORE were developed, with the former involving 10-12 flights per year to make extensive measurements of the atmosphere using state of the art instruments and the latter providing multiple flights per day across the globe using an automated instrument package mounted on multiple aircraft. Further information about the structure of IAGOS and planned future development can be found in Petzold et al. (2015).

Routine measurements by IAGOS on a global scale over the past 25 years have enabled research into a multitude of Essential Climate Variables (ECVs) (Bokinski et al. 2014) on a time scale that is important in the context of global climate change. This has included temperature trends (Berkes et al. 2017), greenhouse gases including CO₂, CH₄, CO and H₂O (Filges et al. 2015; Filges et al. 2018), climatologies of O₃, CO and H₂O in the Upper Troposphere Lower Stratosphere (UTLS) (Clark et al. 2015; Cohen et al. 2018; Gaudel et al. 2018) and cloud properties measured in-situ (Petzold et al. 2017; Beswick et al. 2015). This paper describes long-term in-situ observations between 2011 and 2018 of Cirrus cloud macrophysical properties, location and frequency.

Cirrus is a broad term to describe high altitude clouds that can have very different origins and properties. The majority of Cirrus in Tropical regions is the result of convective thunderstorm outflow (detraind cloud). In the mid latitudes it is most often associated with storm tracks driven by the sub-polar Jetstream, although cirrus from thunderstorm outflow can also be seen over mid latitude continents during the summer months. Contrails formed by the hot moist exhaust products from jet engines can spread into Cirrus and are one of the most visible anthropogenic influences on the global radiation budget (Jones et al. 2012) and the only man-made ice clouds (Kärcher, 2018). The global mean cover produced by these man-made line shaped contrails has been reported to be about 0.1% (Sassen et al., 2008), resulting in a global and annual mean radiative forcing of 0.02 W m⁻² (Minnus et al., 1999). This estimation is subject to large uncertainties with Fahey et al. (1999) reporting a likely range between 0.005 to 0.06 W m⁻² for present day forcing.

Cirrus clouds cover large parts of the globe. In mid-latitudes these high ice clouds cover 30 % at any given time and in the tropics this can be 60-80 % (Baran et al. 2012). The radiative impact of Cirrus clouds is one of the largest sources of uncertainty in global climate models (GCMs) due to the complex microphysical processes that are poorly understood and difficult to measure. The magnitude and even sign of the net radiative effect is very sensitive to these complexities that include properties such as the ice crystal size distribution, the ice crystal shape and the horizontal and vertical extent of the cloud (Petzold et al. 2017; Boucher et al. 2013). Estimations of the radiative effect of these clouds is further complicated when considering the anthropogenic impact on their properties in the future due to changes in the chemical and physical properties of aerosol particles and atmospheric dynamics as a result of a changing climate. Kärcher (2017) suggested that microphysical and macrophysical representation of cirrus in GCMs must be advanced before we can accurately predict their impact on the global climate.

A major source of the uncertainty surrounding Cirrus clouds is the challenging nature of measurements on the relevant scale that capture the evolution and dissipation of these clouds (Krämer et al. 2016, Krämer et al. 2020). Initially the climatological record of Cirrus cloud relied on observations as part of weather records before satellites were developed to detect high altitude ice clouds on a global scale (Sassen et al. 2008). Targeted science projects with research aircraft together with the deployment of ground based remote sensing technology (Sassen and Mace, 2002) have provided detailed information about key cloud parameters including Ice Water Content (IWC), Ice Number Concentration (N_{ice}) and Ice Supersaturation (RH_{ice}). Many of these projects are described in Kramer et al. (2016), Krämer et al. (2020) and Lawson et al. (2019).

Depending on the measurement approach the accurate quantification of cirrus properties is subject to a number of limitations. Ground based observations are limited in their distribution and can be obscured by low cloud. Targeted research flights, despite having sophisticated instrumentation, are limited in their spatial extent. The biggest spatial coverage of cirrus measurements is via space borne remote sensing techniques. However despite the large amount of remote sensing data collected from space it should be cautioned that there are still many challenges with this approach (Sassen, Wang and Liu et al. 2008). In situ-measurements on a relevant scale are needed to characterise cirrus properties and to validate the co-existing measurement techniques. The approach described here sits between existing measurement techniques, providing the large spatial coverage of in-situ measurements that aren't provided by targeted research flights and measuring the size and number density range of cirrus particles that is problematic for satellite remote sensing techniques.

We present the largest in-situ cirrus dataset collected to date, both in terms of the quantity and global coverage of data. We present 79 months of in-situ cloud measurements from the IAGOS fleet of commercial Airbus aircraft on a global scale before focusing on identifiable seasonal trends in different regions.

The focus of this study is on the Upper Troposphere Lower Stratosphere (UTLS) region split into box domains covering the North Atlantic (45-60N 11-53W), Continental Europe (43-53N 22E-1W), the Sub Tropical Atlantic (44-28N 11-53W), the Tropical Atlantic (2S-13N 18-43W), North America (36-60N 71-89W) and South East Asia (5-20N 120-100E).

2 Measurements

Measurements of cloud microphysical properties were made as part of the IAGOS-CORE package of instrumentation on Airbus A330 and A340 aircraft. A fleet of 10 aircraft and 6 international airlines (Air France, Cathay Pacific, China Airlines, Hawaiian Airlines, Iberia and Lufthansa) made more than 8 years of flights. Measurements of the concentration of cloud particles with equivalent optical diameter (EOD) between 5 and 75 μm were made with a Backscatter Cloud Probe (BCP) mounted on the aircraft fuselage. The instrument (Fig. 1a-b) uses a linearly polarized laser (wavelength 658 nm) to detect the backscatter signal from particles that transit through the sample volume. The intensity of this signal is related to the particle size and is used to calculate the concentration of particles detected in flight. Extensive details about the instrument, its calibration and comparison with other instruments and the uncertainties associated with derived particle properties can be found in the technical paper by Beswick et al. (2014). A limitation of the measurements compared to those used on research aircraft however is the lack of identification of possible concentration artefacts due to ice crystal shattering possibly generated by upstream superstructures, (Korolev & Field, 2015). To this end concentration trends are compared as far as possible with near concurrent geo-located measurements from research aircraft, e.g. Petzold et al. (2017) and potential outliers removed from the analyses. We examined cloud measured during the cruise altitude of the aircraft (≥ 10 km).

While we selected flight data above the 10 km altitude level, the operational ceiling of commercial aircraft means our measurements are limited to an altitude range between 10 km and approximately 12.5 km. In some regions, such as the tropics, cirrus clouds are present at altitudes exceeding this altitude (up to ~ 17 km). The capability of the BCP instrument also means larger ice particles in aged cirrus clouds are potentially missed, while very thin cirrus containing few small ice particles might also not be detected (see Petzold et al. 2017 and Krämer et al. 2020).

2.1 Global Measurement Distribution

Figure 2 shows the global distribution of BCP measurements (1 degree resolution) at high altitude (≥ 10 km) over 79 months between December 2012 and July 2018. This shows that the measurements are extensive across the globe from 43 S to 77 N, with the greatest frequency of measurements focussed on commercial air routes over Europe, Africa, across the Atlantic to North and South America, with another focus of activity on SE Asia. The total hours of flight are shown in figure 3 with favoured routes having 10s or even 100s of hours of measurement points. In total this measurement approach has provided over 60,000 hours of measurement data.

2.2 Cloud Fractions

Figure 4 shows the global cloud fraction of clouds ≥ 10 km by the BCP binned by latitude and longitude (1 degree bin resolution). It shows clear regional differences in cloud fraction with higher cloud fractions in regions such as the Inter Tropical Convergence Zone (ITCZ) over the South Atlantic and in SE Asia. In contrast flight paths over the North Atlantic have much lower cloud fractions. The grey colour on figure 1b represents a zero cloud fraction that is produced when the BCP has measured no concentrations of cloud particles $\geq 0.05 \text{ cm}^{-3}$.

The cloud fraction was calculated by taking each 4 second measurement report from the BCP and flagging cloud as present when the reported concentration was $\geq 0.05 \text{ cm}^{-3}$. This low concentration threshold represents 12 detection events and a 30% sampling error. (sampling Data points were considered cloud free when this threshold was not met). The cloud fraction was then calculated as the number of in-cloud points / the number of points in each bin.

2.3 Seasonal Trends in Cloud Fractions

Figure 4. shows the annual global cloud fraction as measured by the BCP on the IAGOS fleet. Based on information about seasonality in different areas of the globe we selected 6 regions for further analysis. The Oceanic regions of the North and Sub Tropical Atlantic were selected to look at the seasonal changes in cloud fraction that are driven by the jet stream storm belts in the mid-latitudes (Wylie et al. 1994). The North Atlantic high cloud amount is strongly influenced by these seasonal changes, the Sub Tropical Atlantic was selected for a contrast to the oceanic regions further towards the poles to investigate high cloud changes with increasing distance towards the equator.

The ITCZ marks the ‘meteorological equator’ where surface trade winds converge to produce a zone of increased mean convection, cloudiness and precipitation (Waliser and Jiang, 2015). The line of convection shifts with the seasons, moving northwards during the northern hemisphere spring and summer, and southwards during the southern hemisphere spring and summer. The large convective systems produce broad areas of cirrus from convective outflow and we selected two regions to examine this band of activity; the tropical Atlantic and SE Asia.

The remaining regions, Europe and North America, were chosen for their continental influence and mid latitude position. This allowed us to look at the relative contributions from the northern hemisphere autumn and winter time jet stream together with high cloud produced by convective outflow during the summer months.

2.3.1 Seasonal Trends in Cloud Fraction by Region

Here we present 6 regions and calculate cloud fraction by season. These regions are described and highlighted on figure. 4. The seasons are split into December, January, February (DJF), March, April May (MAM), June, July August (JJA) and September, October, November (SON). The global map shows the 1 degree binned annual cloud fraction value, the grey colours represent areas in which measurements were made but no cloud was observed. The black boxes enclose the domains that were selected for further analysis by season. The bar charts surrounding the global map represent cloud fraction split by season for each region.

High cloud fraction over Continental Europe was found to be strongly seasonal (fig. 4a). During the northern hemisphere autumn (SON) and winter months (DJF) cloud fractions shows the strongest signal with domain mean cloud fractions of 0.01 and 0.008 for SON and DJF respectively. After the winter cloud fraction drops significantly during MAM before rising again in the JJA period to 0.006.

Over the North Atlantic The cloud fraction (fig. 4d) exhibits a strong signal during the SON and DJF periods. The peak cloud fraction value is during SON with a value of 0.005. The lowest cloud fraction is observed in MAM.

The subtropical Atlantic (fig. 4e) also had a peak cloud fraction (0.014) during SON. During the remaining periods DJF, MAM and JJA cloud fractions are <0.004 with the minimum value recorded during the JJA period (0.001).

North America peak cloud fractions (fig. 4c) occur in the summer (JJA) with values of 0.007. There is also increased cloud fractions during the autumn (SON). The lowest fractions are seen during MAM.

Trends in South East Asia (fig. 4b) are less pronounced but have a peak during the JJA and SON periods of 0.09 and 0.07 respectively. The lowest cloud fractions are observed during MAM.

The Tropical Atlantic region is dominated by the convective activity produced by the ITCZ. In comparison with regions of the globe further towards the poles the cloud fractions are higher in all seasons (fig. 4f). However, our data still exhibits trends through the 4 seasons, with MAM showing the greatest cloud fraction values. The lowest cloud fractions were observed during SON.

3. Discussion

Contributions to the understanding of global cirrus cloud properties has evolved over time from observational reporting at the surface to remote sensing from both space borne and ground based instrumentation designed to study the key microphysical and macrophysical properties of cirrus clouds. In addition to remote sensing techniques, relatively small scale but highly targeted in-situ measurements have vastly improved our understanding of the small scale processes governing cirrus cloud formation, evolution and radiative properties (Kramer et al., 2016). Whilst these targeted airborne research campaigns cover a range of different meteorological conditions, these may not necessarily provide a statistically representative distribution of cirrus cloud frequencies and properties in the UTLS region. To address this long-term global satellite remote sensing is the ideal approach, however retrievals of cirrus microphysical properties can have limitations including altitude resolution and ice crystal number concentrations, which remain a challenge (Sassen et al., 2008). IAGOS is an opportunity to add to the global cirrus climatology, and here we describe some of the initial results from this global in-situ dataset.

We selected our 6 regions to identify seasonal trends in the high-altitude cloud. Figure 4 identifies these regions and the calculated cloud fractions associated with each marked on the map. A key feature of the mid latitudes in the Northern Hemisphere was the signature of increasing cloud fractions in the autumn (SON) and winter (DJF) months. The maritime North Atlantic (fig. 4b) showed this trend the most strongly, with significant increases in these periods and much lower cloud fractions in the spring and summer. The driving force for these changes is the strengthening of the polar vortex during the Northern Hemisphere winter and the storm tracks

that this produces across the North Atlantic. This trend was also evident over Continental Europe (fig. 4c). In addition to this there was also a trend to increasing cloud fractions during the summer period (JJA), presumably due to convective activity over the land producing cirrus from thunderstorm outflow.

The North American region (fig. 4a), although showing the signature of the jet stream driven cirrus in the winter months, was dominated by higher cloud fractions during the summer, likely to be a result of the strong thunderstorm systems that develop over the United States of America (USA) during this season and the associated convective cirrus outflow. The Sub Tropical Atlantic (fig. 4d) had a jet stream cirrus signature during Autumn, but the trend overall was less evident than for the North Atlantic region, which is expected as the distance from the polar front increases and the impact from mid-latitude depressions decreases.

The tropical regions of the Atlantic and South East Asia both exhibited relatively high cloud fractions when compared to the mid latitude continents and oceanic regions. The outflow cirrus in these regions is very dominant, coinciding with the monsoon season in South East Asia but evident the whole year. Over the Tropical Atlantic the outflow cirrus is most likely to be associated with the ITCZ.

The cloud fractions presented for each region were the result of an approach that averages the data from each of the seasons between December 2011 and July 2018. When we examined individual years we found significant inter-annual variability in cloud fractions. While caution should be taken about the measurement bias (data collection focused on busy air corridors) the variability in some regions may represent large scale cyclical climate phenomenon. One example is the El Niño Southern Oscillation (ENSO), a key driver of weather patterns over the tropical Pacific ocean region. Although the annual cycle is most dominant at all longitudes and latitudes Eleftheratos et al. (2011) found that ENSO has a strong influence on Cirrus Cloud Cover (CCC) in the Western Pacific, with 6.2% of the variance explained by ENSO. The contribution to variability by other known cycles that influence weather patterns, such as the QBO, 11 year solar cycle and long-term-trend-related cloud components was estimated to about 1.0%, 0.1% and 0.3% respectively.

The SE Asia region exhibited a significant increase in cirrus cloud fraction during 2016 centred around the JJA and SON period (fig. 5.). Although our measurement period is limited in the context of the ENSO signal this is consistent with findings reported by Virts and Wallace (2010) that found a shift in peak cloudiness towards the maritime continent during La Nina.

In the mid-latitude regions we studied, drivers of cloudiness is also dominated by the seasonal cycle, while large scale dynamics such as the North Atlantic Oscillation also contribute to the inter-annual variability. Eleftheratos et al. (2007) found a small positive correlation between cloud cover in the North Atlantic Flight Corridor (NAFC) of 0.3. They also found trends in cloud cover of +1.6% per decade, demonstrating the importance of continued long-term monitoring of this region.

The aim of this paper was to examine whether the increasingly expansive dataset is representative in a climatological context. We have found common identifiable trends in our

data, particularly the northern hemisphere winter jet stream and the relatively higher cloud fractions in tropical areas attributable to cirrus outflow from thunderstorm outflow. While targeted research flights provide very detailed in-situ measurements of cirrus properties and satellite remote sensing activity gathers data on a global scale, IAGOS and the utilisation of commercial aircraft provides unique opportunities to fill the gap and provide in-situ measurements over large areas of the globe.

4 Conclusions

To conclude, we have presented a global dataset of cloud particle number collected as part of IAGOS. We report a number of key findings.

- We examined regions of the globe covering oceanic, continental and tropical areas to see how representative the dataset was in demonstrating common seasonal trends in each region.
- We found the measurements were able to demonstrate seasonal changes in cloud fraction associated with the northern hemisphere mid latitude jet stream and the relatively higher cloud fractions found in tropical regions as a result of thunderstorm cirrus outflow.
- This dataset and the ongoing measurements as part of IAGOS are an important addition to the already existing infrastructure for monitoring of high-altitude clouds that include remote sensing (ground based and space borne) and targeted research flights.
- The measurements also provide an excellent tool for the aviation industry to investigate the influence of adverse conditions on aircraft performance.

Acknowledgments, Samples, and Data

The data supporting this paper can be obtained via the IAGOS online data portal <http://www.iagos-data.fr/portal.html>

References

- Baran, A. J. (2012). From the single-scattering properties of ice crystals to climate prediction: A way forward. *Atmospheric Research*, 112, 45–69.
<https://doi.org/10.1016/j.atmosres.2012.04.010>
- Berkes, F., Neis, P., Schultz, M. G., Bundke, U., Rohs, S., Smit, H. G. J., et al. (2017). In situ temperature measurements in the upper troposphere and lowermost stratosphere from 2

- decades of IAGOS long-term routine observation. *Atmospheric Chemistry and Physics*, 17(20), 12495–12508. <https://doi.org/10.5194/acp-17-12495-2017>
- Beswick, K., Baumgardner, D., Gallagher, M., Volz-Thomas, A., Nedelec, P., Wang, K. Y., & Lance, S. (2014). The backscatter cloud probe-a compact low-profile autonomous optical spectrometer. *Atmospheric Measurement Techniques*, 7(5), 1443–1457. <https://doi.org/10.5194/amt-7-1443-2014>
- Beswick, Karl, Baumgardner, D., Gallagher, M., Raga, G. B., Minnis, P., Spangenberg, D. A., et al. (2015). Properties of small cirrus ice crystals from commercial aircraft measurements and implications for flight operations. *Tellus B: Chemical and Physical Meteorology*, 67(1), 27876. <https://doi.org/10.3402/tellusb.v67.27876>
- Bojinski, S., Verstraete, M., Peterson, T. C., Richter, C., Simmons, A., & Zemp, M. (2014). The concept of essential climate variables in support of climate research, applications, and policy. *Bulletin of the American Meteorological Society*, 95(9), 1431–1443. <https://doi.org/10.1175/BAMS-D-13-00047.1>
- Clark, H., Sauvage, B., Thouret, V., Nédélec, P., Blot, R., Wang, K., et al. (2015). Tellus B : Chemical and Physical Meteorology The first regular measurements of ozone , carbon monoxide and water vapour in the Pacific UTLS by IAGOS The first regular measurements of ozone , carbon monoxide and water vapour in the Pacific UTLS by IAGOS, 0889.
- Cohen, Y., Petetin, H., Thouret, V., Marécal, V., Josse, B., Clark, H., et al. (2018). Climatology and long-term evolution of ozone and carbon monoxide in the upper troposphere-lower stratosphere (UTLS) at northern midlatitudes, as seen by IAGOS from 1995 to 2013. *Atmospheric Chemistry and Physics*, 18(8), 5415–5453. <https://doi.org/10.5194/acp-18-5415-2018>
- Eleftheratos, K., Zerefos, C. S., Zanis, P., Balis, D. S., Tselioudis, G., Gierens, K., & Sausen, R. (2007). A study on natural and manmade global interannual fluctuations of cirrus cloud cover for the period 1984-2004. *Atmospheric Chemistry and Physics*, 7(10), 2631–2642. <https://doi.org/10.5194/acp-7-2631-2007>
- Eleftheratos, K., Zerefos, C. S., Varotsos, C., & Kapsomenakis, I. (2011). Interannual variability of cirrus clouds in the tropics in el niño southern oscillation (ENSO) regions based on international satellite cloud climatology project (ISCCP) satellite data. *International Journal of Remote Sensing*, 32(21), 6395–6405. <https://doi.org/10.1080/01431161.2010.510491>
- Filges, A., Gerbig, C., Chen, H., Franke, H., Klaus, C., & Jordan, A. (2015a). The IAGOS-core greenhouse gas package: a measurement system for continuous airborne observations of CO₂, CH₄, H₂O and CO. *Tellus B: Chemical and Physical Meteorology*, 67(1), 27989. <https://doi.org/10.3402/tellusb.v67.27989>
- Filges, A., Gerbig, C., Chen, H., Franke, H., Klaus, C., & Jordan, A. (2015b). The IAGOS-core greenhouse gas package: A measurement system for continuous airborne observations of CO₂, CH₄, H₂O and CO. *Tellus, Series B: Chemical and Physical Meteorology*, 6(1). <https://doi.org/10.3402/tellusb.v67.27989>
- Filges, A., Gerbig, C., Rella, C. W., Hoffnagle, J., Smit, H., Krämer, M., et al. (2018). Evaluation of the IAGOS-Core GHG package H₂O measurements during the DENCHAR airborne inter-comparison campaign in 2011. *Atmospheric Measurement Techniques*, 11(9), 5279–5297. <https://doi.org/10.5194/amt-11-5279-2018>
- Gaudel, A., Cooper, O. R., Ancellet, G., Barret, B., Boynard, A., Burrows, J. P., et al. (2018).

- Tropospheric Ozone Assessment Report: Present-day distribution and trends of tropospheric ozone relevant to climate and global atmospheric chemistry model evaluation. *Elementa*, 6. <https://doi.org/10.1525/elementa.291>
- Jones, H. M., Haywood, J., Marenco, F., O'Sullivan, D., Meyer, J., Thorpe, R., et al. (2012). A methodology for in-situ and remote sensing of microphysical and radiative properties of contrails as they evolve into cirrus. *Atmospheric Chemistry and Physics*, 12(17), 8157–8175. <https://doi.org/10.5194/acp-12-8157-2012>
- Kärcher, B. (2017). Cirrus Clouds and Their Response to Anthropogenic Activities. *Current Climate Change Reports*, 3(1), 45–57. <https://doi.org/10.1007/s40641-017-0060-3>
- Kärcher, B. (2018). Formation and radiative forcing of contrail cirrus. *Nature Communications*, 9(1), 1–17. <https://doi.org/10.1038/s41467-018-04068-0>
- Korolev, A., & Field, P. R. (2015). Assessment of the performance of the inter-arrival time algorithm to identify ice shattering artifacts in cloud particle probe measurements. *Atmospheric Measurement Techniques*, 8(2), 761–777. <https://doi.org/10.5194/amt-8-761-2015>
- Krämer, M, Rolf, C., Spelten, N., Afchine, A., Fahey, D., Jensen, E., et al. (2020). A Microphysics Guide to Cirrus – Part II : Climatologies of Clouds and Humidity from Observations. *Atmospheric Chemistry and Physics Discussions*, (January). <https://doi.org/https://doi.org/10.5194/acp-2020-40>
- Krämer, Martina, Rolf, C., Luebke, A., Afchine, A., Spelten, N., Costa, A., et al. (2016). A microphysics guide to cirrus clouds-Part 1: Cirrus types. *Atmospheric Chemistry and Physics*, 16(5), 3463–3483. <https://doi.org/10.5194/acp-16-3463-2016>
- Lawson, R. P., Woods, S., Jensen, E., Erfani, E., Gurganus, C., Gallagher, M., et al. (2019). A Review of Ice Particle Shapes in Cirrus formed In Situ and in Anvils. *Journal of Geophysical Research: Atmospheres*, 124(17–18), 10049–10090. <https://doi.org/10.1029/2018JD030122>
- Minnis, P., Schumann, U., Doelling, D. R., Gierens, K. M., & Fahey, D. W. (1999). Global distribution of contrail radiative forcing. *Geophysical Research Letters*, 26(13), 1853–1856. <https://doi.org/10.1029/1999GL900358>
- Petzold, A., Thouret, V., Gerbig, C., Zahn, A., Brenninkmeijer, C. A. M., Gallagher, M., et al. (2015). Global-scale atmosphere monitoring by in-service aircraft - current achievements and future prospects of the European Research Infrastructure IAGOS. *Tellus, Series B: Chemical and Physical Meteorology*, 6(1), 1–24. <https://doi.org/10.3402/tellusb.v67.28452>
- Petzold, A., Krämer, M., Neis, P., Rolf, C., Rohs, S., Berkes, F., et al. (2017). Upper tropospheric water vapour and its interaction with cirrus clouds as seen from IAGOS long-term routine in-situ observations. *Faraday Discuss.* <https://doi.org/10.1039/C7FD00006E>
- Sassen, K., Wang, Z., & Liu, D. (2009). Global distribution of cirrus clouds from CloudSat/cloud-aerosol lidar and infrared pathfinder satellite observations (CALIPSO) measurements. *Journal of Geophysical Research Atmospheres*, 114(8), 1–12. <https://doi.org/10.1029/2008JD009972>
- Schröder, F., Kärcher, B., Durore, C., Ström, J., Petzold, A., Gayet, J. F., et al. (2000). On the transition of contrails into cirrus clouds. *Journal of the Atmospheric Sciences*, 57(4), 464–480. [https://doi.org/10.1175/1520-0469\(2000\)057<0464:OTTOCI>2.0.CO;2](https://doi.org/10.1175/1520-0469(2000)057<0464:OTTOCI>2.0.CO;2)
- Virts, K. S., & Wallace, J. M. (2010). Annual, interannual, and intraseasonal variability of tropical

tropopause transition layer cirrus. *Journal of the Atmospheric Sciences*, 67(10), 3097–3112.
<https://doi.org/10.1175/2010JAS3413.1>

Wylie, D. P., Menzel, W. P., Woolf, H. M., & Strabala, K. I. (1994). Four years of global cirrus cloud statistics using HIRS. *Journal of Climate*. [https://doi.org/10.1175/1520-0442\(1994\)007<1972:FYOGCC>2.0.CO;2](https://doi.org/10.1175/1520-0442(1994)007<1972:FYOGCC>2.0.CO;2)



Figure 1. (a) Instrument installation on the IAGOS instrumented Airbus and (b) the Backscatter Cloud Probe (BCP).

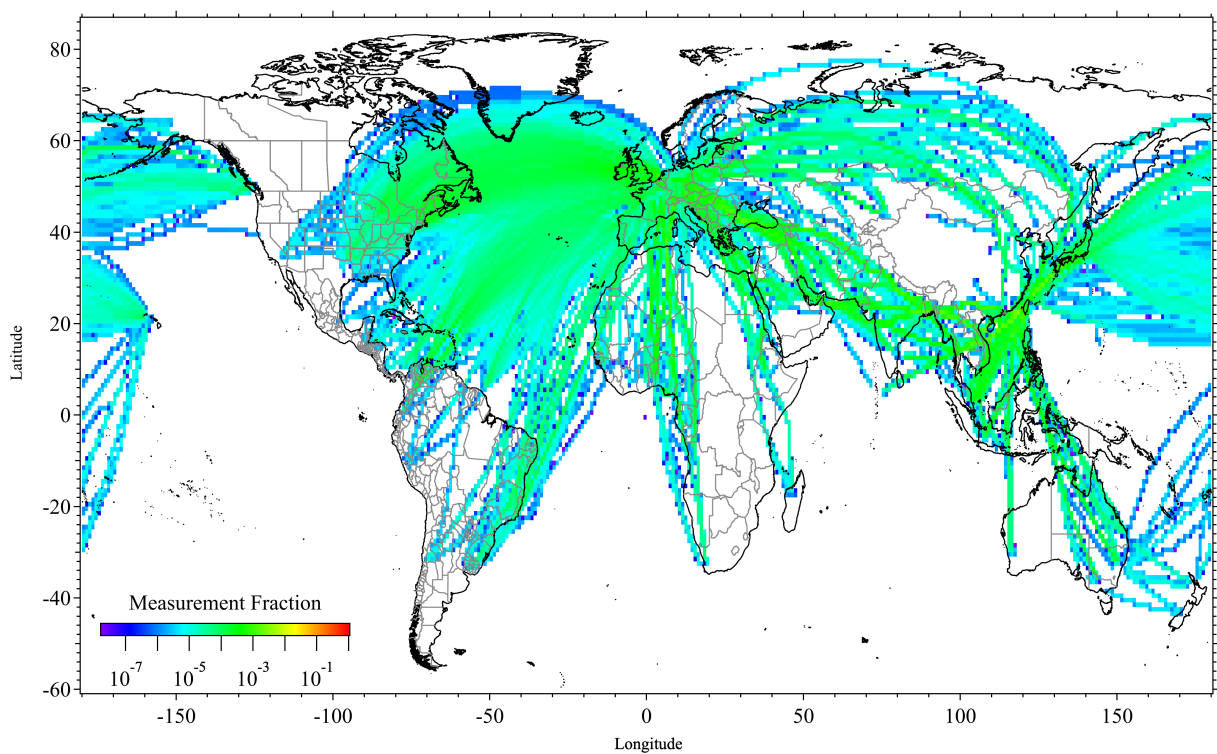


Figure 2. Global measurement fraction from the Backscatter Cloud Probe on the IAGOS fleet of Airbus aircraft.

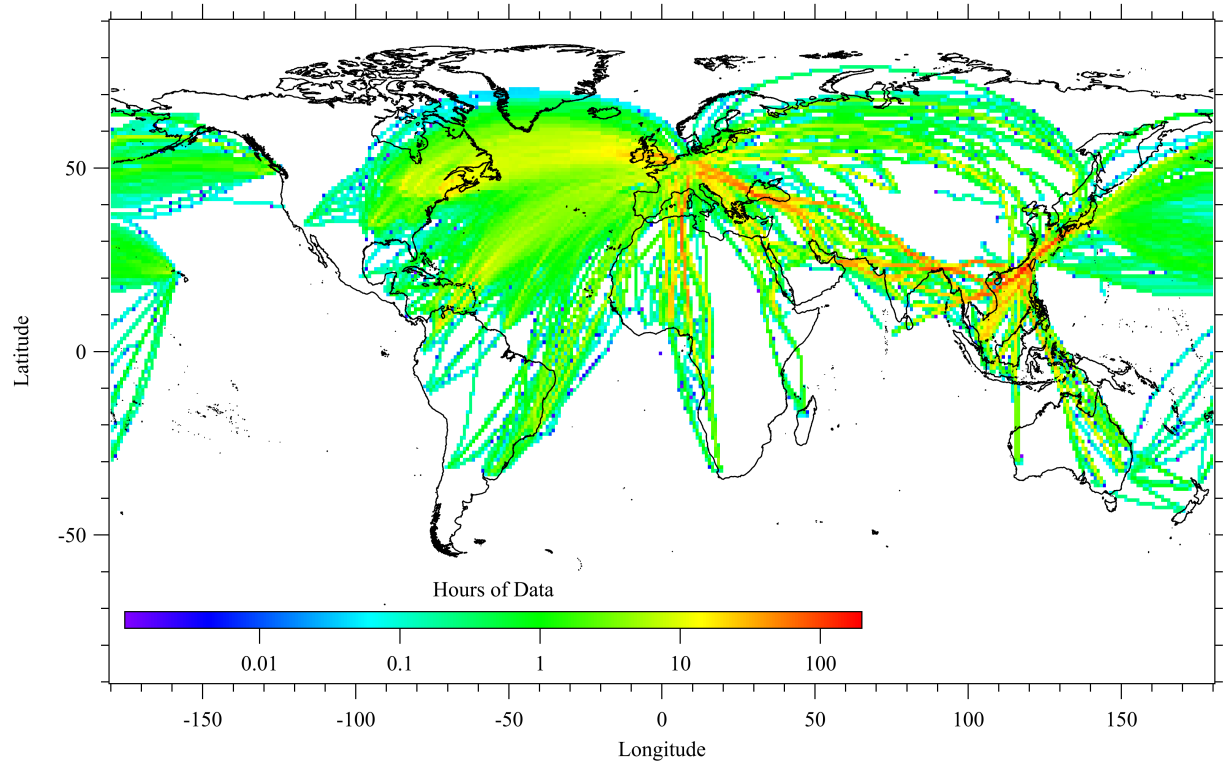


Figure 3. Global measurement hours by the Backscatter Cloud Probe on the IAGOS fleet of Airbus aircraft.

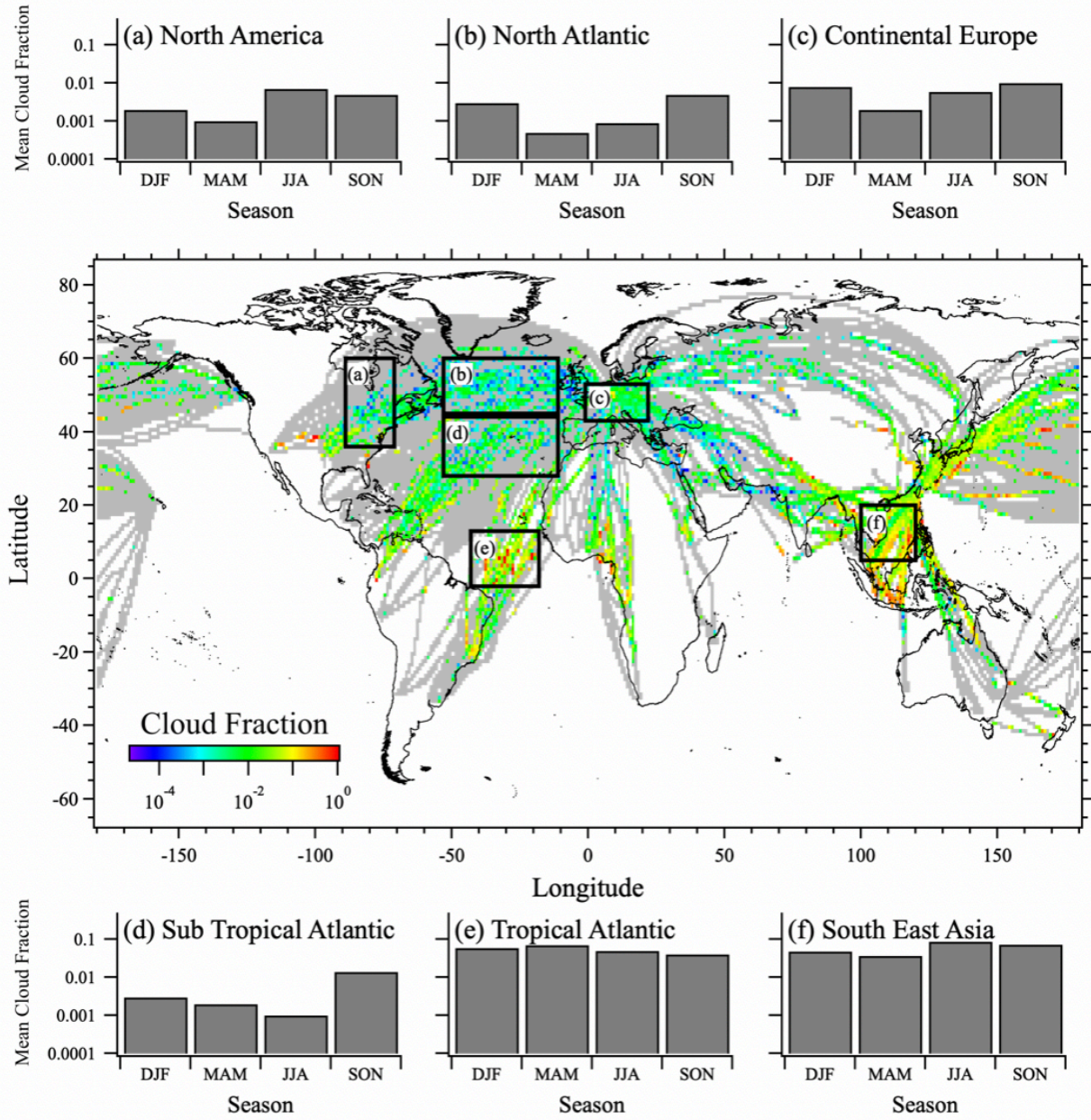


Figure 4. Global cirrus cloud fraction and seasonal mean cirrus cloud fractions for 6 regions

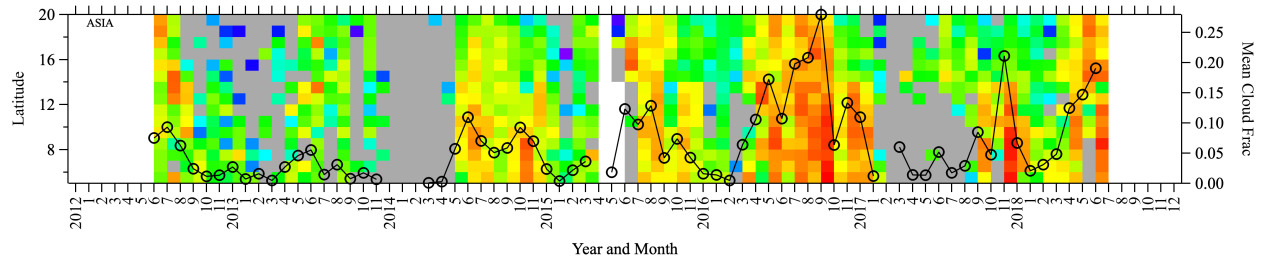


Figure 5. Hövmoller diagram for the period 2012 – 2018 for the Asia region showing monthly latitudinal averaged cirrus cloud fraction and monthly averaged cirrus cloud fraction for the entire region.